Accepted Manuscript

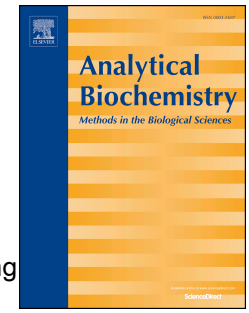

Highly sensitive and selective uric acid biosensor based on a 3D graphene foam/ indium tin oxide glass electrode

Hong Yan Yue, Dr., Professor, Hong Zhang, Jing Chang, Xin Gao, Shuo Huang, Long Hui Yao, Xuan Yu Lin, Er Jun Guo

PII: S0003-2697(15)00345-0

DOI: 10.1016/j.ab.2015.07.007

Reference: YABIO 12143

To appear in: *Analytical Biochemistry*

Received Date: 15 May 2015

Revised Date: 9 July 2015

Accepted Date: 10 July 2015

Please cite this article as: H.Y. Yue, H. Zhang, J. Chang, X. Gao, S. Huang, L.H. Yao, X.Y. Lin, E.J. Guo, Highly sensitive and selective uric acid biosensor based on a 3D graphene foam/indium tin oxide glass electrode, *Analytical Biochemistry* (2015), doi: 10.1016/j.ab.2015.07.007.

Highly sensitive and selective uric acid biosensor based on a 3D graphene foam/indium tin oxide glass electrode

Hong Yan Yue[1,*], Hong Zhang[1], Jing Chang[1], Xin Gao[1], Shuo Huang[2], Long Hui Yao[1], Xuan Yu Lin[1], Er Jun Guo[1]

[1]School of Materials Science and Engineering, Harbin University of Science and Technology, Harbin 150040, People's Republic of China

[2]Department of Neurology, The First Affiliated Hospital of Harbin Medical University, Harbin 150001, People's Republic of China

* Corresponding author

Hong Yan Yue, Dr., Professor

School of Materials Science and Engineering,

Harbin University of Science and Technology,

Harbin 150040, P.R. China.

Email: hyyue@hrbust.edu.cn

Tel: +86-451-86392258

Abstract

A 3D continuous and interconnected network graphene foam (GF) was synthesized by chemical vapor deposition using nickel foam as a template. The morphologies of the GF were observed by scanning electron microscopy. X-ray diffraction and Raman spectroscopy were used to investigate the structure of GF. The graphene with few layers and defect free was closely coated on the backbone of the 3D nickel foam. After etching nickel, the GF was transferred onto indium tin oxide (ITO) glass, which acted as an electrode to detect uric acid using cyclic voltammetry (CV) and differential pulse voltammetry (DPV). The GF/ITO electrode showed a high sensitivity for the detection of uric acid about 9.44 $mA \cdot mM^{-1}$ in the range of 25 nM to 0.1 μM and 1.85 $mA \cdot mM^{-1}$ in the range of 0.1 to 60 μM. The limit of detection of GF/ITO electrode for uric acid is 3 nM. The GF/ITO electrode also showed a high selectivity for the detection of uric acid in the presence of ascorbic acid. This electrode will have a wide range of potential application prospect in electrochemical detection.

Keywords: Chemical vapor deposition; Nickel foam; Graphene foam; Uric acid; Ascorbic acid; Biosensor

1. Introduction

Uric acid (UA) is a very important biological molecule in higher primates and humans (blood: 0.1~0.5 mM, urine: 2 mM). It is a weak organic acid which exists mainly as a monosodium salt under physiologic conditions. Usually, UA can be irreversibly oxidized in aqueous solution and allantoin (ALL) is the major product [1, 2]. Extreme abnormalities of UA levels are symptoms of many diseases including pneumonia, gout and fatal hyperuricemic nephropathy [3]. Ascorbic Acid (AA) is an anti-oxidant which exists in many vegetables, fruits and biological fluids (blood: 0.1 mM, urine 0.6 mM). AA in the body fluids is related to several diseases, such as cancer, diabetes mellitus and hepatic disorders.

Electrochemical methods have been proved to be a very promising way to detect UA and AA by virtue of the electroactive nature of biomolecules. Generally, UA and AA coexist in biological fluids, such as blood and urine. However, UA and AA are oxidized at potentials which are very close to each other and result in overlapped voltammetric responses at conventional solid electrodes [4]. A futuristic requirement for prognosis and diagnosis of disease is just to have a drop of blood instead of a cylinder of blood that is required in the current routine of health test, and further to provide an immediate report and diagnosis to patients. Therefore, it is important to develop a simple, realiable and effective electrode to selectively and sensitively detect

UA in the presence of AA in routine analysis [5-7].

Graphene is a one-atom-thick planar sheet of sp^2-boned carbn atoms which are densely packed in a honey comb crystal lattice [8]. It shows remarkable electrocatalytic and sensing properties due to its high intrinsic carrier mobility and large surface area [9]. Since it is discovered in 2004 [10, 11], it has been extensively investigated in biosensors.

Graphene can be achieved by several techniques, such as micromechanical exfoliation of graphite [12], chemical oxidation of graphite followed by exfotiation and oxygen elimination [13] and chemical vapor deposition (CVD) onto transition metal substrates (typically Ni and Cu) [14, 15]. Among all the methods, chemically derived graphene has been widely adopted because of low cost and large-scale production of grapheme. However, this integrated graphene shows poor electrical conductivity and high contact resistance owing to serious structural defects in graphene sheets introduced during exfoliation and reduction process. CVD is a promising and readily accessible approach to prepare high quality and defect-free graphene with outstanding electrical conductivity. A single to fewer layer continuous graphene films grown onto a nickel film deposited on an oxidized silicon wafer via CVD was used to detect various biological molecules [16]. However, it is limited for the improvement of biomolecule detection by the effective surface area due to the

planar electrode.

In this work, a GF with a 3D continuous and interconnected network was prepared on nickel foam by CVD. When the nickel was etched, the 3D GF was transferred onto ITO glass, acting as the working electrode to detect UA and AA. The 3D GF/ITO electrode demonstrates a high sensitivity for the detection of UA and selective determination of UA in the presence of AA.

2. Experimental

2.1 Chemicals and Reagents

Nickel foam was supplied by Alantum Advanced Technology Materials Co., Ltd (China). ITO glass (specific resistance of < 10 Ω, Zhuhai Kaivo Electronic Co., Ltd, China) was used for the fabrication of electrodes. UA, AA, phosphate buffered saline (PBS) and poly (methyl methacrylate) (PMMA) were purchased from Sigma-Aldrich. Ethyl lactate was purchased from Tokyo Chemical Industry. Deionized water was obtained by purification through a Water Purifier (Sichuan Woter Water Treatment Equipment Co., Ltd, China). 37% HCl and acetone were achieved from Beijing Chemical Company (China).

2.2 Synthesis of 3D GF and electrode

Nickel foam was used as the 3D template for the growth of GF. The growth of a few layers of graphene on the nickel foam by CVD has been reported elesewhere

[17,18]. In brief, the nickel foam was reduced with H_2 flow (200 sccm) at 1010 ℃ for half an hour before the CVD growth (gas ratio of CH_4:H_2=20:200). After etching nickel, the obtained GF (1 cm×1 cm) was transferred onto ITO glass, acting as the electrode, to detect UA and AA.

2.3 Characterizations of 3D GF

The morphologies of 3D GF were observed on a field-emission scanning electron microscope (FESEM, JSM7000F, JEOL) with an accelerating voltage of 20 kV. The structure of GF was investigated by X-ray diffraction (XRD) (Rigaku Rotaflex D/MAX Sestem, Rigaku) with Cu Kα radiation (λ= 0.15406 nm). Raman spectrum was recorded using a micro-Raman system (Renishaw, RM-1000 In via) with an excitation wavelength of 514 nm at room-temperature.

2.4 Electrochemical Measurements

Electrochemical measurements were performed in a 0.1 M PBS solution (pH 7.4) in a three-electrode cell using a VMP3 electrochemical workstation (Biologic Science instrument, France). An Ag/AgCl electrode and a platinum wire respectively acted as the reference electrode and the counter electrode, while the 3D GF/ITO electrode served as the working electrode. The area of the GF/ITO electrode is 0.7 cm^2. Cyclic voltammetry (CV) experiments were carried out at a scan rate of 50 mV s^{-1}. Differential pulse voltammetry (DPV) responses were recorded over a potential range

of -0.2 to 0.6 V with the parameters as previously reported [18].

3. Results and Discussion

3.1 Preparation and characterizations of 3D GF

Figure 1 shows the schematic of the 3D GF/ITO electrode preparation procedures and redox reactions of UA and AA at GF/ITO electrode. The 3D macroporous and inter-connected nickel foam is used as the template to prepare GF by CVD. After removal of nickel, GF retains the morphology of nickel foam. The prepared GF is transferred onto the surface of ITO glass, acting as the electrode, to detect UA and AA. The overall oxidation process of UA and AA biomolecules at GF/ITO electrode is proton dependent and the electron transfer is accompanied by the transfer of an equal number of protons [19]. After oxidation of UA and AA, the electrons are rapidly transferred to the GF/ITO electrode.

The preparation and SEM images of GF are shown in Figure 2. Nickel foam is put into a tube furnace to prepare GF by CVD, as shown in Figure 2a. After growth of graphene, the color of the nickel foam was changed from shiny white to dark gray (Figure 2b). Nickel foam used in this experiment is 3D macroporous structure with an average pore diameter about 100-200 μm (Figure 2c). After growth of graphene and etching of nickel, the GF replicates the 3D structure of nickel foam well without collapse and the surface of the prepared graphene is almost transparent (Figure 2d).

XRD pattern and Raman spectrum of the GF are shown in Figure 3. There are two significant diffraction peaks at 26.5 and 54.7^{o} (Figure 3a) attributed to the (002) and (004) reflections of graphite, respectively (JCPDS 75-1621) [20]. As shown in Figure 3b, two prominent characteristic peaks at ~1580 and 2680 cm^{-1}, corresponding to the G and 2D band of graphene, respectively. The intensity ratio of the G and 2D band indicates that the GF is made up of few layers graphene. In addition, the lack of D band at ~1350 cm^{-1} suggests that the GF is high quality and defect free [21].

3.2 CV Responses of GF/ITO electrode for UA and AA

Figure 4 shows the CV curves of the 3D GF/ITO electrode in 1 mM UA and AA at a scan rate of 50 mV s^{-1}, respectively. ITO electrode is as the comparation. The results indicate for GF/ITO electrode, the oxidation peak potential of UA and AA is ~ 0.3 and 0 V, respectively. For ITO electrode, the oxidation peak potential of UA and AA shows a broad range at ~ 0.45 and 0.35 V, respectively. The GF/ITO electrode shows a significantly higher peak oxidation current than ITO electrode. This may attribute to that the porous 3D GF with a large specific surface area is benefit to the access of biomolecules. In addition, the oxidation peak of GF/ITO electrode for UA and AA is relatively narrow, indicating that GF provides a rapid pathway for electron transportation. The current of oxidation peak is apparently higher than that of the reduction peak, indicating that the redox reaction of UA at GF/ITO electrode is

irreversible. And the reduction peak of AA cannot be observed, illustrating that the redox reaction of AA at GF/ITO electrode is completely irreversible.

CV curves of the GF/ITO electrode in 1 mM UA at different scan rates from 10 to 100 mV s^{-1} are shown in Figure 5a. With increasing the scan rate, the UA oxidation peak current increases and the oxidation peak potential gradually shifts to the positive value. In addition, the oxidation peak current vs. the square root of the scan rate exhibits a linear relationship (Figure 5b), suggesting a diffusion-controlled process [22]. The linear regression equation is Ip (mA) = 0.013 + 0.116 $\upsilon^{1/2}$ (mV) (R=0.996).

3.3 DPV Responses of GF/ITO electrode for UA and AA

DPV method is employed to obtain better sensitivity owing to the enhanced analytical signal obtained by removing the non-Faradic current compared to CV method [23]. Figure 6a shows the DPV curves of the GF/ITO electrode for UA in the range from 25 nM to 60 μM. And the corresponding magnified parts of the electrode for UA in the range of 25 nM to 1 μM are shown in Figure 6b. Two different linear relationships between oxidation peak currents and UA concentration are shown in the inset of Figure 6b. The linear regression equation is I_{UA} (μA) =1.26 + 9.44 C_{UA} (μM) (R=0.927) in the range of 25 nM to 0.1 μM and I_{UA} (μA) =2.07+1.85 C_{UA} (μM) (R=0.989) in the range of 0.1 μM to 1 μM, respectively. The measured limit of detection (m-LOD) and calculated limit of detection (c-LOD) of the GF/ITO electrode

for UA is 25 nM and 3 nM, respectively, which is much smaller than previous reports summarized in Table 1.

The DPV responses of the GF/ITO electrode in UA with different concentrations in the presence of 50 μM AA are shown in Figure 7a. Figure 7b shows a linear relationship of the oxidation peak currents and UA concentrations. The results indicate that the addition of AA does not significantly influnce the oxidation peak currents and peak potential of UA. Therefore, it is potential to selectively, sensitively detect UA in the presence of AA.

3.4 Reproducibility and stability of GF/ITO electrode

To evaluate the reproducibility of the GF/ITO electrode, the peak currents of 20 successive measurments by DPV in 50 μM UA were determined. The relative standard deviation (RSD) was about 1.9 %, indicating that the GF/ITO electrode has an excellent reproducibility. The long-term stability of the electrode was evaluated by measuring its DPV response of 50 μM UA in 0.1 M PBS every 2 days. When not used, the electrode was stored at room temperature under normal condition, and finally 92% of the initial current reponse remained even after two weeks. The result indicates the GF/ITO electrode has a good stability. Thus, the GF/ITO electrode may be a promising candidate for electroanalysis applications.

3.5 Determination of UA in UA injection solutions and human urine samples

UA injection and human urine samples were selected as real biological samples for analysis using the standard addition method. All samples were diluted with 0.1M PBS before measurment. As shown in Table 2, the results indicated that the recoveries of the spiked samples were in the range of 98.9-100.7%. Therefore, the proposed method may provide a feasible tool for determination of UA in real samples. The representative diagnostic detection of UA from human urine in the hospital is commonly used enzyme reaction based spectrophotometric method (or colorimetric method). The results of UA in UA injection solutions and human urine samples is also shown in Table 2.

4. Conclusions

3D GF has been successfully synthesized using nickel foam as a template by CVD. GF is transferred onto ITO glass, acting as an electrode, to detect UA in the presence of AA. The results show that GF has a continuous and interconnected 3D network structure similar to nickel foam. The 3D GF/ITO electrode can selectively detect UA in the presence AA with a higher sensitivity and lower limit of detection. It will show potential applications in electrochemical sensors and biosensor in the future.

Acknowledgements

This work is supported by the National Natural Science Foundation of China (51201052), Science Funds for the Young Innovative Talents of HUST (201306),

Postdoctoral Initial Founding of Heilongjiang Province (LBH-Q1260) and Scientific Research Fund of Heilongjiang Provential Education Department (12541120).

References

[1] J. P. Hart, Ellis Horwood, New York, USA, Chichester, 1990, p.51.

[2] F. Qu, H. Sun, S. Zhang, J. You, M. Yang, Electrochim. Acta 61 (2012) 173-178.

[3] F. Scheller, F. Schubert, D. Pfeiffer, I. Dransfeld, R. Renneberg, U. Wollenberger, K. Riedel, M. Pavlova, M. Kühn, H.G. Müller, P.M. Tan, W. Hoffmann, W. Moritz, Analyst, 114 (2012) 653-661.

[4] B.J. Privett, J.H. Shin, M.H. Schoenfisch, Anal. Chem., 82 (2010) 4723-4741.

[5] G.F. Wang, J. Meng, H.Y. Liu, S.F. Jiao, W. Zhang, D.L. Chen, B. Fang, Electrochim. Acta, 53 (2008) 2837-2843.

[6] Y. Zhang, G.M. Wen, Y.H. Zhou, S.M. Shuang, C. Dong, M.M.F. Choi, Biosens. Bioelectron., 22 (2007) 1791-1797.

[7] D. Lakshmi, M.J. Whitcombe, F. Davis, P.S. Sharma, B.B. Prasad, Electroanal., 23 (2011) 305-320.

[8] R.A. Brazhe, A.I. Kochaev, Phys. Solid State, 54 (2012) 1612-1614.

[9] S.M.M. Dubois, Z. Zanoli, X. Declerck, J.C. Charlier, Eur. Phys. J. B, 72 (2009) 1-24.

[10] S. Hussain, M.W. Iqbal, J. Park, M. Ahmad, J. Singh, J. Eom, J. Jung, Nanoscale Res. Lett., 9 (2014) 546-549.

[11] M.S. Xu, Y. Gao, H.Z. Chen, Chinese Sci. Bull., 57 (2012) 3000-3009.

[12] R.C. Haddon, Accounts Chem. Res., 46 (2013) 2191-2192.

[13] G.D. Semchenko, I.Y. Shuteeva, O.N. Slepchenko, L.A. Anglenko, Refract. Ind. Ceram., 46 (2005) 260-267.

[14] R.S. Edward, K.S. Coleman, Accounts Chem. Res., 46 (2013) 23-30.

[15] D.C. Wei, B. Wu, Y.L. Guo, G. Yu, Y.Q. Liu, Accounts Chem. Res., 46 (2013) 106-115.

[16] D.A.C. Brownson, M. Gómez-Mingot, C.E. Banks, Phys. Chem. Chem. Phys., 13 (2011) 20284-20288.

[17] Z. P. Chen , W.C. Ren , L.B. Gao , B.L. Liu , S.F. Pei , H.M. Cheng. Nat. Mater. 10 (2011) 424-428.

[18] S. Huang, H.Y. Yue, J. Zhou, J.J. Zhang, C.Y. Zhang, X. Gao, J. Chang. Electroanal., 26 (2014) 184-190.

[19] X.F. Liu, L. Zhang, S.P. Wei, S.H. Chen, X. Ou, Q.Y. Lu, Biosens. Bioelectron., 57 (2014) 232-238.

[20] Y.H. Ding, H.M. Ren, F.H. Chang, P. Zhang, Y. Jiang, Bull. Mater. Sci., 36 (2013) 1073-1077.

[21] A. Bello, K. Makgopa, M. Fabiane, D. DODOO-Ahrin, K.I. Ozoemena, N. Manyala, J. Mater. Sci., 48 (2013) 6707-6712.

[22] Y. Ding, Y. Wang, L. Su, M. Bellagamba, H. Zhang, Y. Lei, Biosens. Bioelectron., 26 (2010) 542-548.

[23] M. Hadi, A. Rouhollahi, Anal. Chim. Acta, 721 (2012) 55-60.

[24] S.A. Kumar, H.W. Cheng, S.M. Chen, Electroanal., 21 (2009) 2281-2286.

[25] F. Ni, Y.L. Wang, D. Zhang, F. Gao, M. Li, Electroanal., 22 (2010) 1130-1135.

[26] G. Wang, J. Meng, H. Liu, S. Jiao, W. Zhang, D. Chen, B. Fan, Electrochim. Acta, 53 (2008) 2837-2843.

[27] J.S. Ye, Y. Wen, W.D. Zhang, L.M. Gan, G.Q. Xu, F.S. Sheu, Electroanl., 15 (2013) 1693-1698.

[28] F. Zhang, X. Wang, S. Ai, Z. Sun, Q. Wan, Z. Zhu, Y. Xian, L. Jin, K. Yamamto, Anal. Chim. Acta, 519 (2004) 155-160.

List of Figure and Table Captions

Figure 1 Schematic of the preparation procedures of 3D GF/ITO electrode and redox reactions of UA and AA at GF/ITO electrode.

Figure 2 Preparation and SEM images of GF. **a**, Photographs of nickel foam (3 cm x 10 cm) for GF growth and CVD chamber. **b**, Photographs of nickel foam (down) and graphene grown on nickel foam (up). **c**, SEM image of nickel foam. **d,** SEM image of GF after etching nickel.

Figure 3 Structural analysis of GF. **a**, XRD patterns of GF. **b**, Raman spectrum of GF.

Figure 4 CV curves of GF/ITO electrcode in UA and AA at a scan rate of 50 mV s^{-1}. **a**, CV curves of GF/ITO and ITO electrode in 1 mM UA. **b**, CV curves of GF/ITO and ITO electrode in 1 mM AA.

Figure 5 CV curves of GF/ITO electrode in 1 mM UA at different scan rates. **a**, Scan rates are 10, 25, 50, 75 and 100 mV s^{-1}; **b**, Relationship of the oxidation peak currents of UA versus the square-root of the scan rate .

Figure 6 DPV measurements of GF/ITO electrode in UA. **a**, UA concentrations from bottom to top: 0.0025, 0.05, 0.1, 0.25, 0.5, 0.75, 1, 2.5, 5, 10, 20, 40 and 60 μM; **b**, Corresponding magnified part of Figure 6a. UA concentrations from bottom to top: 0.0025, 0.05, 0.1, 0.25, 0.5, 0.75 and 1 μM. Inset: Relationship of the oxidation peak currents versus UA concentrations. DPV conditions: pulse height: 50 mV; pulse width: 200 ms; step height: 4 mV; step time: 500 ms.

Figure 7 DPV measurements of GF/ITO electrode in the mixed UA and AA. **a**, 50 μM AA and UA concentrations from bottom to top: 1, 2.5, 5, 10, 20, 40 and 60 μM; **b**, Relationship of the oxidation peak currents of UA versus UA concentrations. The DPV conditions are the same as in Figure 6.

Table 1 Summary of previously published results for detection of UA by DPV using different electrodes.

Table 2 Determination of UA in UA injection solutions and human urine samples with the GF/ITO electrode.

Table 1 Summary of previously published results for detection of UA by DPV using different electrodes.

Electrode	Sensitivity (LDR), μA/μM (μM)	m-LOD (c-LOD), (nM)	Ref.
PL/GCE	0.06(30-1000)	30000(2000)	24
LDHf/GCE	—(2-400)	2000(660)	25
LaHCF/GCE	2.0879(0.2−100)	200(100)	26
MWNTs/GCE	0.61(0.2-80)	200(100)	27
NiO/ZnO/CPE	0.035(12.9-629)	1290(970)	28
	0.001(629-6290)		
GF/ITO	**9.44(0.025-0.1)**	**25(3)**	**Ours**
	1.85(0.1-60)		

LDR: linear dynamic range; m-LOD: measured limit of detection; c-LOD: calculated limit of detection

PL/GCE: polymerized luminol film/glassy carbon electrode

LDHf/GCE: Zn/Al LDH film/glassy carbon electrode

LaHCF/GCE: hexacyanoferrate lanthanum film/glassy carbon electrode

MWNTs/GCE: multiwalled carbon nanotubes/glassy carbon electrode

NiO/ZnO/CPE: NiO/ZnO/glassy carbon electrode

GF/ITO: graphene foam/ITO glass electrode

Table 2 Determination of UA in UA injection solutions and human urine samples with the GF/ITO electrode. (n=5)

Samples	Spiked (μM)	Found (μM)	Recovery (%)	RSD (%)	Colorimetric method
UA injection	10	10.04	100.40	1.4	10.15
	20	20.13	100.65	0.5	20.05
	40	39.88	99.70	2.1	40.05
Urine	10	10.06	100.60	0.4	9.95
	10	10.15	101.50	1.1	10.10
	10	9.89	98.90	0.8	10.05